

See discussions, stats, and author profiles for this publication at: <https://www.researchgate.net/publication/323221015>

# Performance Analysis of Orthogonal Space-Time Block Codes Over Nakagami-q MIMO RFID Backscattering Channels

Article in IET Communications · February 2018

DOI: 10.1049/iet-com.2017.1230

CITATIONS

0

READS

69

2 authors:



Ali Jamoos

Al-Quds University

37 PUBLICATIONS 125 CITATIONS

[SEE PROFILE](#)



Yasmin Qabbani

Al-Quds University

1 PUBLICATION 0 CITATIONS

[SEE PROFILE](#)

Some of the authors of this publication are also working on these related projects:



Expanding Mobile Network Spectrum with Cognitive Radios [View project](#)



Energy Detection in Cognitive Radio Networks [View project](#)

# Performance analysis of orthogonal space-time block codes over Nakagami- $q$ MIMO RFID backscattering channels

 ISSN 1751-8628  
 Received on 2nd November 2017  
 Revised 25th January 2018  
 Accepted on 12th February 2018  
 E-First on 4th May 2018  
 doi: 10.1049/iet-com.2017.1230  
 www.ietdl.org

 Ali Jamoos<sup>1</sup> ✉, Yasmin Qabbani<sup>1</sup>
<sup>1</sup>Department of Electronic and Communication Engineering, Al-Quds University, Jerusalem, Palestine

✉ E-mail: ali.jamoos@staff.alquds.edu

**Abstract:** The authors employ the conditional moment generating function approach to analyse the performance of orthogonal space-time block codes over Nakagami- $q$  (Hoyt) multiple-input multiple-output radio frequency identification backscattering channels. New exact and asymptotic symbol error rate expressions are derived for the case of two and four receiving antennas ( $N = 2, 4$ ). The exact expressions are in the form of a sum of infinite series while the asymptotic ones are in the closed form. The diversity order that the system can achieve is found to be  $L$ , where  $L$  is the number of tag antennas, and the performance of this system is found to be more sensitive to the channel condition (the  $q$  parameter) of the forward link than that of the backscattering link. The theoretical results (exact and asymptotic) are verified through comparison with simulation results.

## 1 Introduction

This radio frequency identification (RFID) is a form of wireless non-contact communication that uses radio waves to automatically identify and track objects [1]. A basic RFID system is made up of three primary components: RFID readers (also known as interrogators), RFID tags, and RFID software or middleware [2]. The tag contains electronically stored information which can be read from up to several metres away in response to reader's interrogating radio waves. Depending on power supplying methods, RFID tags are divided into three categories passive, active, and semi-passive tags [3].

Since passive tags are the least expensive of these three types, they are commonly used in high volumes of applications. For passive RFID tags that draw energy from the reader and simply reflect back a modulated signal to it, the channel between the reader and the tag is the cascade of two fading channels, the forward and backscatter links [4]. This cascaded channel, which is characterised as a query-fading-coding-fading structure, causes deeper and more frequent small-scale fades than the conventional one-way channel resulting in lower transmission reliability and shorter reading ranges [3].

One way to reduce fading in the backscatter channel is through antenna diversity. Ingram *et al.* [5] brought up the idea of increasing the range and communication capacity using multiple radio frequency (RF)-tag and reader antennas. Mi *et al.* [6] also agree that the harvested power required to operate the RF tag chip can be increased by using multiple RF-tag antennas.

Few fading measurements have been conducted and reported in the literature. Fading on the signal received by the RF tag was the focus of Mitsugi and Shibao [7, 8] and Polivka *et al.* [9] studies. Others have studied fading on the signal received by the reader: Kim *et al.* [10] have presented small-scale fading statistics (the cumulative distribution functions) for short ranges in an indoor environment at 2.4 GHz, while Banerjee *et al.* [11, 12] have presented fading measurements at 915 MHz and demonstrated the importance of spatial and frequency diversity to effectively mitigate multipath fading effects.

In an effort to provide a more comprehensive view of the multiple-input multiple-output (MIMO) RF backscattering channel's behaviour, extensive analysis was also performed. In [13–16], researchers provided analytical symbol error rate (SER) expressions and revealed several interesting properties of the channel assuming Rayleigh fading. Others studied the behaviour of the channel under more general fading models. In [17], researchers

analytically investigated the operating range of the MIMO structure under the Nakagami- $m$  fading. The authors in [18] presented a general formulation to study orthogonal space-time block codes (OSTBCs) for RF backscattering with different fading assumptions and then analytically studied the SER performances under Rician fading and Nakagami- $m$  fading using the conditional moment generating function (MGF) approach.

The Nakagami- $q$  model was first introduced by Nakagami [19] as an approximation for the Nakagami- $m$  fading distribution in the range of fading that extends from the one-sided Gaussian model to the Rayleigh model [20]. Recently, this model is being used more frequently in performance analysis of wireless communication systems [21–24], and it shows good ability to describe the statistics of real-world fading channels.

In this study, new exact and asymptotic expressions are derived for the SER performance of the orthogonal space-time block codes over Nakagami- $q$  (Hoyt) MIMO RFID backscattering channels by employing the conditional MGF method. The derived exact expressions are in the form of a sum of infinite series while the asymptotic ones are in the closed form.

The rest of the paper is organised as follows. Section 2 briefly reviews the space-time block code (STBC) system model in a RFID MIMO channel. In Section 3, we analytically study the SER performance of OSTBCs over Nakagami- $q$  fading, where SER expressions are derived. Numerical results are discussed in Section IV. Finally, we draw our conclusions in Section V.

## 2 Passive tag signalling model

In a passive RFID system, a tag modulates its antenna (load-dependent) reflection coefficient  $\Delta(t)$ , which carries out the tag ID, only responsive to receiving an unmodulated RFID signal from the reader, as illustrated in Fig. 1. The MIMO passive channel was first described in [13], as an  $M \times L \times N$  dyadic backscatter channel that represents the propagation of signals in a backscatter radio system consisting of  $M$  transmitters,  $L$  RFID tags, and  $N$  receiver antennas, shown in Fig. 2 [15].

The received signal from the  $M \times L \times N$  dyadic channel (an  $N \times 1$  vector) is given by

$$r(t) = \mathbf{H}^b S(t) \mathbf{H}^f \mathbf{x}(t) + \mathbf{n}(t), \quad (1)$$

Where  $\mathbf{x}(t)$  (an  $M \times 1$  vector) is the unmodulated signals transmitted from the reader,  $\mathbf{n}(t)$  (an  $N \times 1$  vector) is the

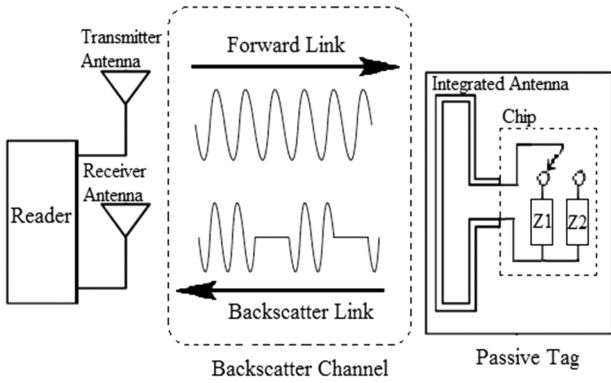


**Fig. 1** RFID reader transmits an unmodulated (query) signal to the RF tag and the RF tag scatters a modulated signal back to the reader, where  $Z_i$  is the impedance corresponding to the reflection coefficient  $\Delta_i(t)$

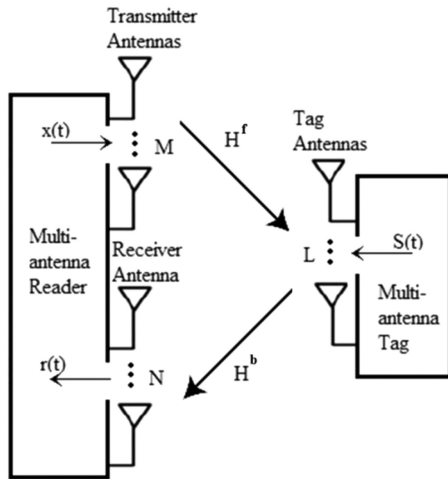


**Fig. 2** Illustration of the MIMO RFID channel signalling scheme. In a passive RFID system, the coding and modulation are done by the tag circuits on the tag side and the reader transmitting antennas actually act as charging devices

corresponding noises at the reader receivers,  $\mathbf{H}^f$  (an  $L \times M$  matrix) is the channel matrix from the reader to the tag,  $\mathbf{H}^b$  (an  $N \times L$  matrix) is the channel matrix from the tag to the reader, and  $\mathbf{S}(t)$  (an  $L \times L$  matrix) is the signalling matrix that describes the time-varying modulation and coding of the carrier signals by the  $L$ -antenna RF tag [25].

In this study, we focus on the case where the tag antennas modulate backscatter with different signals and none of the (modulated) backscattered signals are transferred between these antennas. In this case, the signalling matrix is a diagonal matrix of the form

$$\mathbf{S}(t) = \begin{pmatrix} \Delta_1(t) & & \\ & \ddots & \\ & & \Delta_L(t) \end{pmatrix}, \quad (2)$$

where  $\Delta_l(t)$  denotes the load reflection coefficient of the  $l$ th tag antenna [13]. This matrix with unequal load reflection coefficients can result in space-time codes at the tag end [15].

For our passive RFID system, considering the fact that the reader transmitting-antennas transmit the same query signal from the  $M$  antennas and that the forward channel gains are independent Gaussian, if the total transmitted energy is normalised to unity, the forward channel statistics will be the same for any  $M$ . So from this time on, we will only focus on the  $1 \times N \times L$  channel and we will call it the  $N \times L$  channel for simplicity.

Now, let  $\mathbf{s} = (s_1, \dots, s_L)^T = (\Delta_1(t), \dots, \Delta_L(t))^T$  denote the  $L$  transmission symbols simultaneously transmitted from  $L$  tag

antennas, we can alternatively express the received signal vector at a particular time point as

$$\mathbf{r} = \mathbf{H}\mathbf{s} + \mathbf{w}, \quad (3)$$

where  $\mathbf{H}$  is the channel matrix of the  $N \times L$  channel and can be expressed as

$$\mathbf{H} = \begin{pmatrix} h_1^f h_{1,1}^b & h_2^f h_{2,1}^b & \dots & h_L^f h_{L,1}^b \\ \vdots & \ddots & \ddots & \vdots \\ h_1^f h_{1,N}^b & h_2^f h_{2,N}^b & \dots & h_L^f h_{L,N}^b \end{pmatrix}, \quad (4)$$

where  $h_l^f$ 's ( $l = 1, \dots, L$ ) represent forward channels of the  $N \times L$  channel,  $h_{l,n}^b$ 's ( $l = 1, \dots, L$ ), ( $n = 1, \dots, N$ ) represent backscattering channels,  $h_l^f$  and  $h_{l,n}^b$  are assumed to be statistically independent of each other [13]. Sub-channels  $h_l^f$  and  $h_{l,n}^b$  follow certain fading distribution depending on the propagation environment.

### 3 SER performance of OSTBC for MIMO RF backscattering channels

Among space-time coding schemes, OSTBC is one of the most attractive ones because it is able to provide full diversity gain without channel state information at transmission and with very simple encoding and decoding procedures. Here, a quick review of the general conditional MGF approach used to study OSTBCs for the RF backscattering channel [18] is given, before employing it to analyse the OSTBC over the Hoyt RFID backscattering channel.

#### 3.1 Conditional MGF approach

The probability density function (PDF) approach is a widely used approach to evaluate the SER performance of different wireless channels. For the RF backscattering channel case because of its complex query-fading-coding-fading structure, applying this approach is not preferable. Alternatively, He and Wang [18] proposed the conditional MGF approach, as described next.

Due to its orthogonality property, OSTBC can be transformed from the MIMO fading channel in (3) to the following  $M$  parallel single-input-single-output channels [26]:

$$\hat{r} = \sqrt{\|\mathbf{H}\|_F^2} \hat{s} + \hat{\mathbf{w}}, \quad (5)$$

where  $\|\mathbf{H}\|_F^2 = \sqrt{\sum_{n=1}^N \sum_{l=1}^L |h_l^f h_{l,n}^b|^2}$  is the Frobenius norm of  $\mathbf{H}$ ,  $\hat{\mathbf{s}} = (\hat{s}_1, \dots, \hat{s}_M)^T$  represents the  $M$  incoming symbols, and each element of  $\hat{\mathbf{w}} = (\hat{w}_1, \dots, \hat{w}_M)^T$  is complex Gaussian distributed with zero mean and unit variance. In addition,  $\hat{\mathbf{r}} = (\hat{r}_1, \dots, \hat{r}_M)^T$  represent the received symbols that can be detected based on a simple maximum-likelihood method.

Let  $E_b$  denotes the average energy per bit and  $E_s$  denotes the average energy per symbol, then  $E_s = E_b \log_2 K$  where  $K$  is the size of the signal constellation. The instantaneous signal-to-noise ratio (SNR) per symbol is therefore given by  $\gamma = ((\|\mathbf{H}\|_F^2 \log_2 K)/R)/(E_b/N_0) = ((\|\mathbf{H}\|_F^2 \log_2 K)/R)\bar{\gamma} = \|\mathbf{H}\|_F^2 g \bar{\gamma}$ , where  $R = M/T$  means the symbol rate and we define  $g = \log_2 K/R$ .

The SER of OSTBC can be calculated by averaging the density of  $\|\mathbf{H}\|_F^2$  over  $Q(g\bar{\gamma} \|\mathbf{H}\|_F^2)$  as follows:

$$P_{\text{OSTBC}}(\bar{\gamma}) = E_{\mathbf{H}}(Q(\sqrt{g\bar{\gamma}}\|\mathbf{H}\|_F)) = \frac{1}{\pi} \int_{\theta=0}^{\pi/2} G(\bar{\gamma}) d\theta. \quad (6)$$

Here, the alternative representation of the  $Q$  function as in [27] is employed, and  $\bar{\gamma} = (g\bar{\gamma}/\sin^2\theta)$ ,  $G(\bar{\gamma}) = E_{\mathbf{H}}(\exp(-g\bar{\gamma}\|\mathbf{H}\|_F^2/\sin^2\theta))$  means the MGF of  $\|\mathbf{H}\|_F^2$ .

To find  $G(\bar{\gamma})$ , we define

$$\|\mathbf{H}\|_F^2 = \sum_{l=1}^L \|\mathbf{H}_l\|_F^2 = \sum_{n=1}^N \alpha_l \beta_{l,n} \quad (7)$$

as the squared Frobenius norm of the  $l$ th column of  $\mathbf{H}$ , where  $\alpha_l = |h_l^f|^2$  and  $\beta_{l,n} = |h_{l,n}^b|^2$ . We can see that  $\|\mathbf{H}_l\|_F^2$ 's are independent random variables; therefore, the MGF  $G(\bar{\gamma})$  can be represented as a multiplication of the MGFs of  $\|\mathbf{H}_l\|_F^2$ 's

$$G(\bar{\gamma}) = \prod_{l=1}^L G_l(\bar{\gamma}) \quad (8)$$

If we fix  $\alpha_l$ , the random variable  $\|\mathbf{H}_l\|_F^2 = \alpha_l \sum_{n=1}^N \beta_{l,n}$  is exactly the same as the gain of an  $N$ -branch single-input-multiple-output system with maximum ratio combining at the receiver, with  $N$  branches  $h_{l,n}^b = \alpha_l \beta_{l,n}$  for  $n = 1, \dots, N$ , and each branch has transmission power  $\alpha_l$ . Therefore, we have the MGF  $G_l(\bar{\gamma})$  as

$$G_l(\bar{\gamma}) = \int_0^\infty \prod_{n=1}^N G_{h_{l,n}^b}(\bar{\gamma}) f_{\alpha_l}(\alpha) d\alpha \quad (9)$$

Consequently

$$G(\bar{\gamma}) = \prod_{l=1}^L \left( \int_0^\infty \prod_{n=1}^N G_{h_{l,n}^b}(\bar{\gamma}) f_{\alpha_l}(\alpha) d\alpha \right) \quad (10)$$

where  $f_{\alpha_l}(\alpha)$  is the pdf of  $\alpha_l$  and  $G_{h_{l,n}^b}(\bar{\gamma})$  is the MGF of the conditional distribution of  $h_{l,n}$  on  $\alpha_l$  (i.e. the squared magnitude of the  $l$ th forward channel gain). Next, we employ this approach to find the SER performance under Hoyt fading.

### 3.2 SER of OSTBC over Hoyt RF backscattering channels

Here, we evaluate the SER of OSTBC for the channel assuming  $h_l^f$ 's and  $h_{l,n}^b$ 's are Hoyt fading. For Hoyt fading, the pdf of  $\alpha_l$  is

$$f_{\alpha_l}(\alpha) = \frac{1 + q_f^2}{2q_f} e^{-\frac{(1+q_f^2)\alpha}{4q_f^2}} \sum_{m=0}^{\infty} \frac{1}{(m!)^2} \left( \frac{1 - q_f^4}{8q_f^2} \alpha \right)^{2m} \quad (11)$$

where  $q_f$  is the  $q$  factor of the forward channel. In Hoyt fading, the MGF of  $\beta_{l,n} = |h_{l,n}^b|^2$  is given by [28]

$$G_{\beta_{l,n}}(\bar{\gamma}) = \left( 1 + 2\bar{\gamma} + \frac{q_b^2 (2\bar{\gamma})^2}{(1 + q_b^2)^2} \right)^{(-1/2)} \quad (12)$$

Therefore, the conditional MGF  $G_{h_{l,n}^b}(\bar{\gamma})$  can be obtained by multiplying the SNR of (12) by  $\alpha_l$

$$G_{h_{l,n}^b}(\bar{\gamma}) = \left( 1 + 2\alpha_l \bar{\gamma} + \frac{q_b^2 (2\alpha_l \bar{\gamma})^2}{(1 + q_b^2)^2} \right)^{(-1/2)} \quad (13)$$

where  $q_b$  is the  $q$  factor of the backscattering channel. Substitute  $f_{\alpha_l}(\alpha)$  and  $G_{h_{l,n}^b}(\bar{\gamma})$  into (9), the exact form of  $G_l(\bar{\gamma})$  can be

expressed as in (14) (see Appendix A) (see (14)) where  $k_f = q_f^2$ ,  $k_b = q_b^2$ ,  $k_1 = 1 + k_b$ ,  $k_2 = 1 + k_f$ ,  $D_1 = (1 + k_f)/(2\sqrt{k_f})$ ,  $D_2 = (1 - k_f^2)/(8k_f)$ ,  $D_3 = (4k_b)/(1 + k_b)^2$ , and the function  $M(s, \hat{m}, \hat{N}) = \int_{t=0}^{\infty} t^{\hat{m}-1} e^{-t} (1 + st)^{-\hat{N}} dt$  was well studied in [29] and has the following form:

$$M(s, \hat{m}, \hat{N}) = e^{\frac{1}{s}} s^{-\hat{N}} \sum_{k=0}^{\hat{m}-1} \binom{\hat{m}-1}{k} \left(-\frac{1}{s}\right)^{\hat{m}-k-1} \times \Gamma\left(k - \hat{N} + 1, \frac{1}{s}\right) \quad (15)$$

As the derived expression of the MGF in (14) is complicated with the sum of the infinite series form, asymptotic expressions are usually preferable. Therefore, asymptotically in high (SNR) regimes, it can be shown that (see Appendix A)

$$G_l(\bar{\gamma}) \doteq \begin{cases} \frac{C_{1,2}^f C_{2,2}^b}{2g} \bar{\gamma}^{-1}, & N = 2, \\ \frac{C_{1,4}^f C_{2,4}^b}{g} \bar{\gamma}^{-1}, & N = 4. \end{cases} \quad (16)$$

Substituting (16) into (8) and then into (6) can yield asymptotic expression of SER for OSTBC

$$P_{\text{OSTBC}}(\bar{\gamma}, N, L) \doteq \begin{cases} C_L \left( \frac{C_{1,2}^f C_{2,2}^b}{2g} \right)^L \bar{\gamma}^{-L}, & N = 2, \\ C_L \left( \frac{C_{1,4}^f C_{2,4}^b}{g} \right)^L \bar{\gamma}^{-L}, & N = 4, \end{cases} \quad (17)$$

where  $C_{1,2}^f = (1 + k_f)/(2\sqrt{k_f})$ ,  $C_{2,2}^b = k_1 \ln(k_b)/(k_b - 1)$ ,  $C_{1,4}^f = (1 + k_f)/(2\sqrt{k_f})$ ,  $C_{2,4}^b = (k_1^2/(2(k_b - 1)^2)) - (k_b k_1 \ln(k_b)/(k_b - 1)^3)$  and  $C_L = \Gamma(L + (1/2)) / (2\sqrt{\pi} \Gamma(L + 1))$ .

It should be noted that Appendix A presents the systematic derivation of both the exact and the asymptotic MGF expressions. It was noticed by experimentations that the infinite series in (14) converges rapidly by summing up the first few terms, where the higher terms are negligible. Indeed, it was shown in the derivation of the asymptotic expressions in Appendix A that the terms of the infinite series with  $m > 0$  add zero values to the sum when  $N=2$  whereas the terms with  $m > 0$  can be ignored for high SNR when  $N = 4$ .

## 4 Numerical results and discussion

In this section, the results of the exact and asymptotic expressions for two and four reader-receiving antennas are demonstrated and are compared with simulation results. Figs. 3–6 show the SER curves of the OSTBC scheme with binary phase shift keying (BPSK) modulation in the Hoyt  $N \times L$  MIMO RFID channel for two and four receiving antennas, as well as for different values of the  $q$  factor of the forward and backscattering channels. The upper limit of the infinite series in (14) is set to 5 as higher terms are negligible. According to Figs. 3–6, the asymptotic results are an upper bound of the exact expressions with a perfect match at a high value of SNR. In addition, the simulation results are very close to the theoretical exact results. Two important properties for this

$$G_l(\bar{\gamma}) = \begin{cases} \sum_{m=0}^{\infty} \frac{D_1 D_2^{2m}}{(m!)^2} \left( \frac{D_1^2}{(k_b - 1)} \right)^{-(2m+1)} \left( k_b M\left( \frac{2k_b \bar{\gamma}}{k_1 D_1^2}, 2m+1, 1 \right) - M\left( \frac{2\bar{\gamma}}{k_1 D_1^2}, 2m+1, 1 \right) \right) \\ \sum_{m=0}^{\infty} \frac{D_1 D_2^{2m}}{(m!)^2} \left( \frac{D_1^2}{(k_b - 1)} \right)^{-(2m+1)} \left( (k_b - 1) M\left( \frac{2\bar{\gamma}}{k_1 D_1^2}, 2m+1, 2 \right) - k_b^2 (1 - k_b) M\left( \frac{2k_b \bar{\gamma}}{k_1 D_1^2}, 2m+1, 2 \right) \right. \\ \left. + 2k_b M\left( \frac{2\bar{\gamma}}{k_1 D_1^2}, 2m+1, 1 \right) - k_b^2 M\left( \frac{2k_b \bar{\gamma}}{k_1 D_1^2}, 2m+1, 1 \right) \right), \end{cases} \quad (14)$$

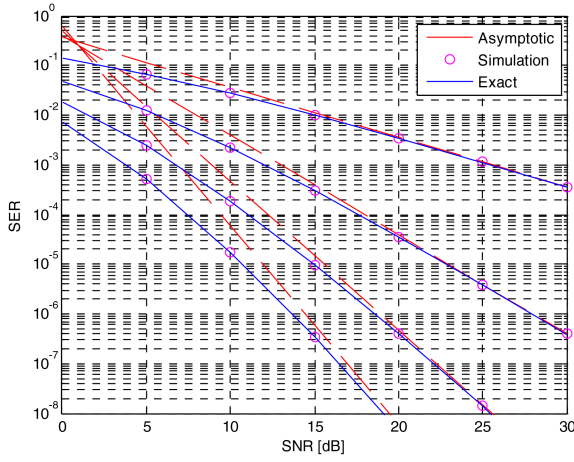


**Fig. 3** SER performances of the RFID channel, with  $q_f = q_b = 0.5$ . From the top to the bottom: ( $L = 1, N = 2$ ), ( $L = 2, N = 2$ ), ( $L = 3, N = 2$ ), ( $L = 4, N = 2$ ), respectively

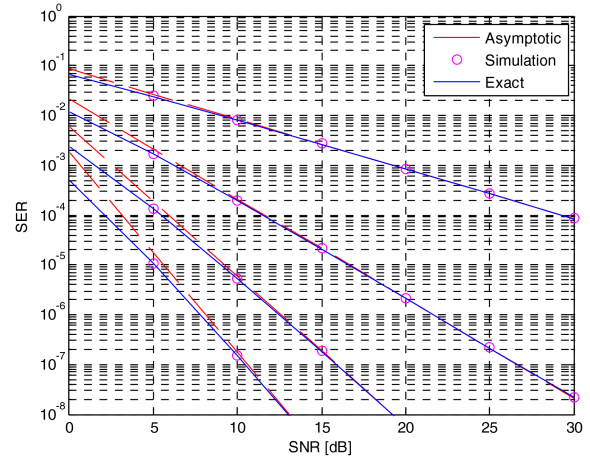


**Fig. 6** SER performances of the RFID channel, with  $q_f = q_b = 0.9$ . From the top to the bottom: ( $L = 1, N = 4$ ), ( $L = 2, N = 4$ ), ( $L = 3, N = 4$ ), ( $L = 4, N = 4$ ), respectively

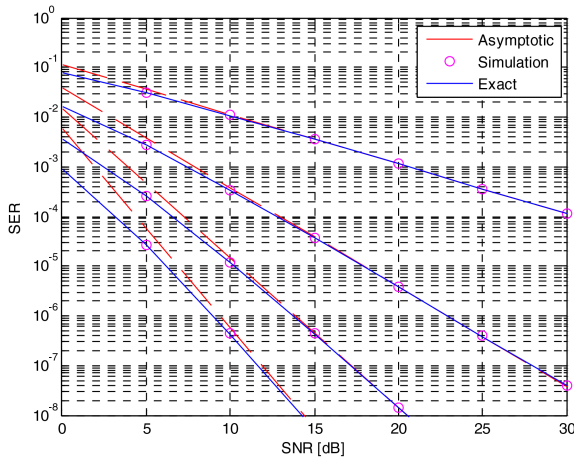


**Fig. 4** SER performances of the RFID channel, with  $q_f = q_b = 0.5$ . From the top to the bottom: ( $L = 1, N = 4$ ), ( $L = 2, N = 4$ ), ( $L = 3, N = 4$ ), ( $L = 4, N = 4$ ), respectively

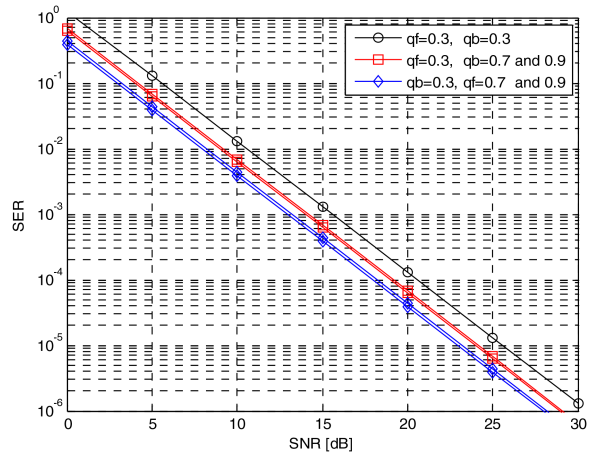


**Fig. 7** When  $q_f = 0.3$  is fixed, the variations of  $q_b$  (0.3, 0.7, and 0.9) do not affect too much the SER; by contrast, when  $q_b = 0.3$  is fixed, the variations of  $q_f$  (0.3, 0.7, and 0.9) change the SER significantly

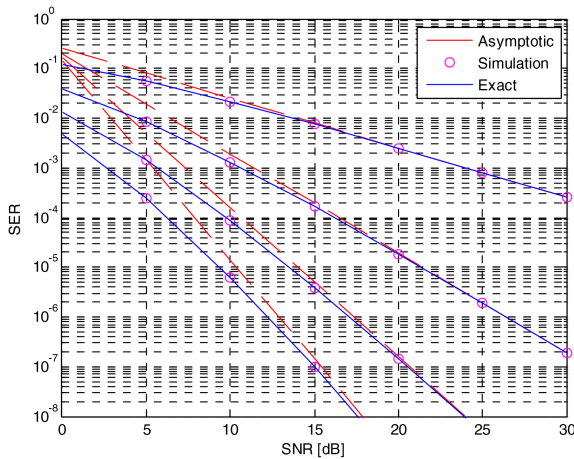


**Fig. 5** SER performances of the RFID channel, with  $q_f = q_b = 0.9$ . From the top to the bottom: ( $L = 1, N = 2$ ), ( $L = 2, N = 2$ ), ( $L = 3, N = 2$ ), ( $L = 4, N = 2$ ), respectively

RFID channel can be discussed: the achievable diversity order and the effects of forwarding and backscattering links on the performance.

(i) *Diversity order*: The diversity order measures how many statically independent copies of the same symbol the receiver is able to separate. When the SNR tends to infinity the slope of bit error rate versus SNR in log-scale shows the diversity order. For

the asymptotic expressions in (17), the asymptotic diversity orders for the Hoyt fading MIMO RF backscattering channel with ( $N = 2$  and 4) are

$$d_a = \lim_{\bar{\gamma} \rightarrow \infty} \left( -\frac{\log P(\bar{\gamma})}{\log \bar{\gamma}} \right) = L. \quad (18)$$

As also observed in Figs. 3–6, where the slopes of these SER curves only depend on  $L$ , the receiving antennas  $N$  does not affect the diversity gain.

(ii) *Impact of forward and backscattering channel conditions*: Another appealing property of the MIMO RF backscattering channel is that the channel condition of the forward link has a more noticeable impact on performance than that of the backscattering link. For Hoyt fading with ( $N = 2, L = 2$ ), Fig. 7 implies that, with  $q_f$  being fixed, changing  $q_b$  does not have a notable effect on the SER curves. Contrarily, with  $q_b$  being fixed, SER curves significantly change when  $q_f$  changes. Fig. 8 shows that similar observations are true for the Hoyt distributed forward and backscattering links with four reader-receiving antennas ( $N = 4, L = 2$ ).

A plot of the asymptotic expressions' coefficients in (17), shown in Fig. 9, perfectly consists of the findings in Figs. 7 and 8, where the effect of the forward channel is reflected by coefficients  $C_{1,2}^f$  and  $C_{1,4}^f$ , and that of the backscattering channel is reflected by  $C_{1,2}^b$  and  $C_{1,4}^b$  for  $N = 2$  and 4, respectively.

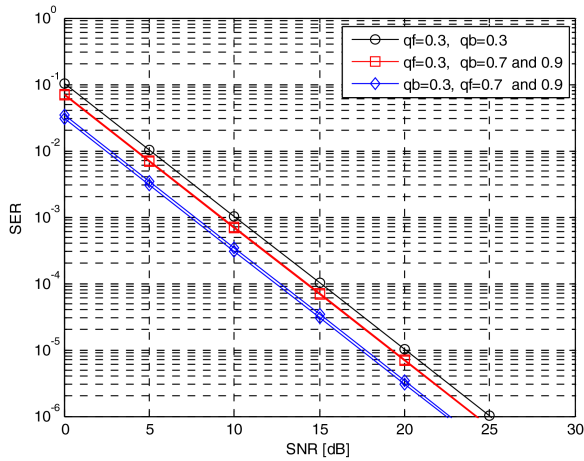


**Fig. 8** When  $q_f = 0.3$  is fixed, the variations of  $q_b$  (0.3, 0.7, and 0.9) do not affect too much the SER; by contrast, when  $q_b = 0.3$  is fixed, the variations of  $q_f$  (0.3, 0.7, and 0.9) change the SER significantly

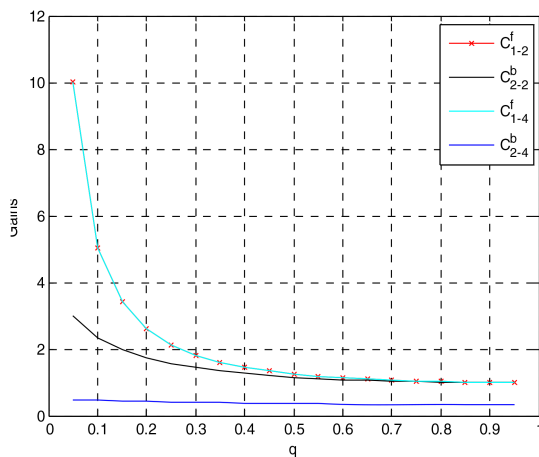


**Fig. 9**  $C^f$  and  $C^b$  are the coefficients in the asymptotic SER related with the forward links and the backscattering links, respectively.  $C^b$  is almost constant as the  $q_b$  increases, whereas  $C^f$  significantly decreases as the  $q_f$  increases

## 5 Conclusion

This study presented a systematic analysis for orthogonal STBCs in MIMO RFID channels under Hoyt fading. Based on this analysis, new SER expressions were derived using the conditional moment generating approach. In particular, exact SER expressions in the form of the sum of infinite series were obtained for two and four receiving antennas ( $N = 2, 4$ ). In addition, asymptotic closed form expressions were also derived. Furthermore, the theoretical exact and asymptotic results are verified with simulation results. Moreover, several interesting properties of the channel were observed from our analytical results. First, the diversity order is solely determined by the number of tag antennas  $L$ . Second, the analytical results reveal that the SER of the MIMO RF channel is much more sensitive to the channel condition of the forward links than that of the backscattering links.

## 6 References

- [1] Want, R.: 'An introduction to RFID technology'. IEEE Pervasive Comput., 2006, pp. 25–33
- [2] Klaus, F.: 'RFID handbook: fundamentals and applications in contactless smart cards and identification' (Wiley, UK, 2003)
- [3] He, C., Wang, Z.J.: 'Unitary query for the  $M \times L \times N$  MIMO backscatter RFID channel', *IEEE Trans. Wirel. Commun.*, 2015, **14**, pp. 2613–2625
- [4] He, C., Wang, Z.J.: 'Impact of the correlation between forward and backscatter channels on RFID system performance'. IEEE Int. Conf. on Acoustics, Speech and Signal Processing, 2011
- [5] Ingram, M., Demirkol, M., Kim, D.: 'Transmit diversity and spatial multiplexing for RF links using modulated backscatter'. Int. Symp. on Signals, Systems, and Electronics, Tokyo, Japan, 2001

- [6] Mi, M., Mickle, M. H., Capelli, C., *et al.*: 'RF energy harvesting with multiple antennas in the same space', *IEEE Antennas Propag.*, 2005, **47**, (5), pp. 100–106
- [7] Mitsugi, J.: 'UHF band RFID readability and fading measurements in practical propagation environment', Auto-ID Labs White Paper Series, 2005, pp. 37–44
- [8] Mitsugi, J., Shibao, Y.: 'Multiplex identification using steepest gradient method for dynamic inventory in UHF RFID'. Int. Symp. on Applications and the Internet, Hiroshima, Japan, 2007
- [9] Polivka, M., Svanda, M., Hudec, P.: 'Analysis and measurement of the RFID system adapted for identification of moving objects'. 36th European Microwave Conf., 2006
- [10] Kim, D., Ingram, M. A., Smith, W.W.: 'Measurements Of small-scale fading and path loss for long range RF tags', *IEEE Trans. Antennas Propag.*, 2003, **51**, (8), pp. 1740–1749
- [11] Banerjee, S.R., Jesme, R., Sainati, R.A.: 'Performance analysis of short range UHF propagation as applicable to passive RFID'. IEEE Int. Conf. on RFID, Grapevine, TX, 2007
- [12] Banerjee, S.R., Jesme, R., Sainati, R.A.: 'Investigation of spatial and frequency diversity for long range UHF RFID'. IEEE Antennas and Propagation Society Int. Symp., San Diego, CA, 2008
- [13] Griffin, J.D., Durgin, G.D.: 'Gains for RF tags using multiple antennas', *IEEE Trans. Antennas Propag.*, 2008, **56**, (2), pp. 563–570
- [14] He, C., Wang, Z.J.: 'Closed-form BER analysis of non-coherent FSK in MISO double Rayleigh fading/RFID channel', *IEEE Commun. Lett.*, 2011, **15**, pp. 848–850
- [15] He, C., He, X., Chen, Z.J., *et al.*: 'On the performance of MIMO RFID backscattering channels', *EURASIP J. Wirel. Commun. Netw.*, 2012, **11**, pp. 1–27
- [16] Boyer, C., Roy, S.: 'Space time coding for backscatter RFID', *IEEE Trans. Wirel. Commun.*, 2013, **12**, (5), pp. 2272–2280
- [17] Kim, D.Y., Jo, H.S., Yoon, H., *et al.*: 'Reverse-link interrogation range of a UHF MIMO-RFID system in Nakagami- $m$  fading channels', *IEEE Trans. Ind. Electron.*, 2010, **57**, (4), pp. 1468–1477
- [18] He, C., Wang, Z.J.: 'SER of orthogonal space-time block codes over Rician and Nakagami- $m$  RF backscattering channels', *IEEE Trans. Veh. Technol.*, 2014, **63**, (2), pp. 654–663
- [19] Nakagami, M.: 'The  $m$ -distribution – a general formula of intensity distribution of rapid fading' in Hoffman, W.G. (ed.): 'Statistical methods in radio wave propagation' (Pergamon Press, Oxford, UK, 1960)
- [20] Youssef, N., Wang, C.X.: 'A study on the second order statistics of Nakagami-Hoyt mobile fading channels', *IEEE Trans. Veh. Technol.*, 2005, **54**, (4), pp. 1259–1265
- [21] Simon, M.K., Alouini, M.S.: 'Digital communication over fading channels' (Wiley-IEEE, USA, 2004)
- [22] Zogas, D.A., Karagiannidis, G.K., Kotsopoulos, S.A.: 'Equal gain combining over Nakagami- $m$  (Rice) and Nakagami- $q$  (Hoyt) generalized fading channels', *IEEE Trans. Wirel. Commun.*, 2005, **4**, pp. 374–379
- [23] Radaydeh, R., Matalgah, M.: 'Non-coherent improved-gain diversity reception of binary orthogonal signals in Nakagami- $q$  (Hoyt) mobile channels', *IET Commun.*, 2008, **2**, (2), pp. 372–379
- [24] Kumbhani, B., Kshetrimayum, R.S.: 'MIMO wireless communications over generalized fading channels' (CRC Press, USA, 2017)
- [25] Zheng, F., Kaiser, T.: 'A space-time coding approach For RFID MIMO systems', *EURASIP J. Embed. Syst.*, 2012, (9), doi: 10.1186/1687-3963-2012-9
- [26] Sandhu, S., Paulraj, A.: 'Space-time block codes: a capacity perspective', *IEEE Commun. Lett.*, 2000, **4**, (12), pp. 384–386
- [27] Stridh, R., Ottersten, B., Karlsson, P.: 'MIMO channel capacity of a measured indoor radio channel at 5.8 GHz'. Thirty-fourth Asilomar Conf. on Signals, Systems and Computers, 2000, vol. 1, pp. 733–737
- [28] Simon, M., Alouini, M.: 'A unified approach to the performance analysis of digital communication over generalized fading channels', *Proc. IEEE*, 1998, **86**, (9), pp. 1860–1877
- [29] Gong, Y., Letiaief, K.: 'On The error probability of orthogonal space-time block codes over keyhole MIMO channel', *IEEE Trans. Wirel. Commun.*, 2007, **6**, pp. 2402–2409

## 7 Appendix

### Evaluation of $P_{\text{OSTBC}}(\bar{\gamma})$

The PDF of the forward channel that follows the Nakagami- $q$  distribution (normalised channel energy) is

$$f(\alpha_l) = \frac{1 + q_l^2}{2q_l} e^{-\frac{(1+q_l^2)\alpha_l}{4q_l^2}} \sum_{m=0}^{\infty} \frac{1}{(m!)^2} \left( \frac{1 - q_l^4}{8q_l^2} \alpha_l \right)^{2m}, \quad (19)$$

where the equality is given by the Taylor expansion of the modified Bessel function of the first kind (i.e.  $I_0(\cdot)$ ). We can expand the conditional MGF  $G_l(\bar{\gamma} | \alpha_l)$  as

$$G_l(\bar{\gamma} | \alpha_l) = \left( \left( 1 + 2 \alpha_l \bar{\gamma} + \frac{q_b^2 (2 \alpha_l \bar{\gamma})^2}{(1 + q_b^2)^2} \right)^{\frac{-1}{2}} \right)^N. \quad (20)$$

Therefore, averaging  $G(\bar{\gamma} | \alpha_l)$  over the density of  $\alpha_l$  gives

$$\begin{aligned} G_l(\bar{\gamma}) &= \int_{\alpha_l=0}^{\infty} f(\alpha_l) G_l(\bar{\gamma} | \alpha_l) d\alpha_l \\ &= \int_{\alpha_l=0}^{\infty} \frac{1 + q_f^2}{2q_f} e^{-\frac{(1+q_f^2)^2 \alpha_l}{4q_f^2}} \sum_{m=0}^{\infty} \frac{1}{(m!)^2} \left( \frac{1 - q_f^4}{8q_f^2} \alpha_l \right)^{2m} \\ &\quad \times \left( 1 + 2 \alpha_l \bar{\gamma} + \frac{q_b^2 (2 \alpha_l \bar{\gamma})^2}{(1 + q_b^2)^2} \right)^{\frac{-N}{2}} d\alpha_l \\ &= \sum_{m=0}^{\infty} \frac{D_1 D_2^{2m}}{(m!)^2} \int_{\alpha_l=0}^{\infty} e^{-D_1^2 \alpha_l} \alpha_l^{2m} \\ &\quad \times \left( 1 + 2 \alpha_l \bar{\gamma} + D_3 (\alpha_l \bar{\gamma})^2 \right)^{(-N/2)} d\alpha_l \\ &\doteq \sum_{m=0}^{\infty} \frac{D_1 D_2^{2m}}{(m!)^2} F(\bar{\gamma}), \end{aligned} \quad (21)$$

where  $k_f = q_f^2$ ,  $k_b = q_b^2$ ,  $k_1 = 1 + k_b$ ,  $k_2 = 1 + k_f$ ,  $D_1 = (1 + k_f)/(2\sqrt{k_f})$ ,  $D_2 = (1 - k_f^2)/(8k_f)$ ,  $D_3 = (4k_b)/(1 + k_b)^2$ , and  $F(\bar{\gamma})$  is defined as follows.

**Case 1:  $N = 2$**

(see (22)), where we use partial fraction expansion to arrive at the second line, and change of variable to arrive at the fourth line,  $y = D_1^2 \alpha_l$ . By letting  $\hat{m} = 2m + 1$  and  $\hat{N} = 1$  we can make use of the function  $M(s, \hat{m}, \hat{N}) \doteq \int_{t=0}^{\infty} t^{\hat{m}-1} e^{-t} (1 + s t)^{-\hat{N}} dt$  that was well studied in [27] and has a closed form of

$$\begin{aligned} M(s, \hat{m}, \hat{N}) &\doteq e^{(1/s)} s^{-\hat{N}} \sum_{k=0}^{\hat{m}-1} \binom{\hat{m}-1}{k} \left( -\frac{1}{s} \right)^{\hat{m}-k-1} \\ &\quad \times \Gamma \left( k - \hat{N} + 1, \frac{1}{s} \right), \end{aligned} \quad (23)$$

where  $\Gamma(\cdot, \cdot)$  is the incomplete gamma function. Substituting (23) in (22) and (21) we obtain (14) for  $N = 2$ .

**Proof of the asymptotic form:** The asymptotic form can be obtained when only considering the terms associated with the lower terms of  $m$  in the exact form. This is because the lower order of the pdf of  $\alpha_l$  determines the asymptotic performance when SNR is large.  $M(s, \hat{m}, \hat{N})$  has an asymptotic form for large  $\bar{\gamma}$  [18]

$$M(s, \hat{m}, \hat{N}) \doteq \begin{cases} \frac{\ln(s)}{s^{\hat{m}}}, & \hat{m} = \hat{N}, \\ \frac{(\hat{m}-1)! (a-b-1)!}{(a-1)! s^b}, & \hat{m} \neq \hat{N}, \end{cases} \quad (24)$$

where  $a = \max(\hat{m}, \hat{N})$  and  $b = \min(\hat{m}, \hat{N})$ . With  $m = 0$ , we have  $\hat{m} = \hat{N} = 1$ , and

$$\begin{aligned} F(\bar{\gamma}) &= \frac{(D_1^2)^{-1}}{(k_b - 1)} \left( k_b M \left( \frac{2k_b \bar{\gamma}}{k_1 D_1^2}, 1, 1 \right) - M \left( \frac{2\bar{\gamma}}{k_1 D_1^2}, 1, 1 \right) \right) \\ &\doteq \frac{(D_1^2)^{-1}}{(k_b - 1)} \left( k_b \frac{\ln \left( \frac{2k_b \bar{\gamma}}{k_1 D_1^2} \right)}{\left( \frac{2k_b \bar{\gamma}}{k_1 D_1^2} \right)} - \frac{\ln \left( \frac{2\bar{\gamma}}{k_1 D_1^2} \right)}{\left( \frac{2\bar{\gamma}}{k_1 D_1^2} \right)} \right) \\ &= \frac{k_1}{2\bar{\gamma} (k_b - 1)} \ln(k_b). \end{aligned} \quad (25)$$

Substitute the asymptotic form of  $F(\bar{\gamma})$  back into (21) we have the asymptotic form of  $G_l(\bar{\gamma})$  as

$$G_l(\bar{\gamma}, m = 0) = \frac{D_1 k_1 \ln(k_b)}{2(k_b - 1)} \bar{\gamma}^{-1}. \quad (26)$$

For  $m > 0$ , we have  $a = \max(\hat{m}, \hat{N}) = \hat{m}$ ,  $b = \min(\hat{m}, \hat{N}) = \hat{N} = 1$  and (see equation below). Therefore, we have  $G_l(\bar{\gamma}, m > 0) = 0$ , and

$$G_l(\bar{\gamma}) \doteq G_l(\bar{\gamma}, m = 0) = \frac{D_1 k_1 \ln(k_b)}{2(k_b - 1)} \bar{\gamma}^{-1}. \quad (27)$$

**Case 2:  $N = 4$**

See (28), where we use partial fraction expansion to arrive at the second line, and change of variable to arrive at the fourth line,  $y = D_1^2 \alpha_l$ . By letting  $\hat{m} = 2m + 1$  and  $\hat{N} = 1$  or 2 depending on the power in each term, we can again make use of the function  $M(s, \hat{m}, \hat{N})$  in (23). Substitute (23) in (28) and (22) we obtain (14) for  $N = 4$ .

**Proof of the asymptotic form:** For  $m = 0$ , we have  $\hat{m} < \hat{N}$  for the first two terms of  $F(\bar{\gamma})$ , and  $\hat{m} = \hat{N}$  for the rest and change of variable to arrive to the fourth line,  $y = D_1^2 \alpha_l$ . (see (28)),

(see (29)). Substitute the asymptotic form of  $F(\bar{\gamma})$  back to (21) we have the asymptotic form of  $G_l(\bar{\gamma})$  as

$$\begin{aligned} F(\bar{\gamma}) &= \int_{\alpha_l=0}^{\infty} e^{-D_1^2 \alpha_l} \alpha_l^{2m} \left( 1 + 2 \alpha_l \bar{\gamma} + D_3 (\alpha_l \bar{\gamma})^2 \right)^{-1} d\alpha_l \\ &= \int_{\alpha_l=0}^{\infty} e^{-D_1^2 \alpha_l} \alpha_l^{2m} \frac{k_1}{(k_b - 1)} \left( \frac{k_b}{(k_1 + 2k_b \bar{\gamma} \alpha_l)} \right) d\alpha_l \\ &\quad - \int_{\alpha_l=0}^{\infty} e^{-D_1^2 \alpha_l} \alpha_l^{2m} \frac{k_1}{(k_b - 1)} \left( \frac{1}{(k_1 + 2\bar{\gamma} \alpha_l)} \right) d\alpha_l \\ &= \left( \frac{k_b}{(k_b - 1)} (D_1^2)^{-(2m+1)} \int_{y=0}^{\infty} \left( 1 + \frac{2k_b \bar{\gamma}}{k_1 D_1^2} y \right)^{-1} e^{-y} y^{2m} dy \right) \\ &\quad - \left( \frac{1}{(k_b - 1)} (D_1^2)^{-(2m+1)} \int_{y=0}^{\infty} \left( 1 + \frac{2\bar{\gamma}}{k_1 D_1^2} y \right)^{-1} e^{-y} y^{2m} dy \right) \\ &= \frac{(D_1^2)^{-(2m+1)}}{(k_b - 1)} \left( k_b \int_{y=0}^{\infty} \left( 1 + \frac{2k_b \bar{\gamma}}{k_1 D_1^2} y \right)^{-1} e^{-y} y^{2m} dy \right) \\ &\quad - \left( \int_{y=0}^{\infty} \left( 1 + \frac{2\bar{\gamma}}{k_1 D_1^2} y \right)^{-1} e^{-y} y^{2m} dy \right), \end{aligned} \quad (22)$$

$$G_i(\bar{\gamma}, m=0) = D_1 \left( \frac{k_1^2}{2(k_b-1)^2} - \frac{k_b k_1 \ln(k_b)}{(k_b-1)^3} \right) \bar{\gamma}^{-1}. \quad (30)$$

For  $m > 0$ , we have  $a = \max(\hat{m}, \hat{N}) = \hat{m}$ ,  $b = \min(\hat{m}, \hat{N}) = \hat{N}$  and see (31).

Therefore, we have (see equation below). The terms for  $m > 0$  can be ignored since  $G_i(\bar{\gamma}, m=0) = o(\bar{\gamma}^{-1}) \gg o(\bar{\gamma}^{-2})$  for large SNR.

Therefore (see (31)).

$$G_i(\bar{\gamma}) \doteq G_i(\bar{\gamma}, m=0) = D_1 \left( \frac{k_1^2}{2(k_b-1)^2} - \frac{k_b k_1 \ln(k_b)}{(k_b-1)^3} \right) \bar{\gamma}^{-1}. \quad (32)$$

$$\begin{aligned} F(\bar{\gamma}) &= \frac{(D_1^2)^{-(2m+1)}}{(k_b-1)} \left( k_b M\left(\frac{2k_b \bar{\gamma}}{k_1 D_1^2}, 2m+1, 1\right) - M\left(\frac{2\bar{\gamma}}{k_1 D_1^2}, 2m+1, 1\right) \right) \\ &= \frac{(D_1^2)^{-(2m+1)}}{(k_b-1)} \left( k_b \frac{(2m-1)!}{\left(\frac{2k_b \bar{\gamma}}{k_1 D_1^2}\right)} - \frac{(2m-1)!}{\left(\frac{2\bar{\gamma}}{k_1 D_1^2}\right)} \right) = 0. \end{aligned}$$

$$\begin{aligned} F(\bar{\gamma}) &= \int_{\alpha_1=0}^{\infty} e^{-D_1^2 \alpha_1} \alpha_1^{2m} (1 + 2\alpha_1 \bar{\gamma} + D_3 (\alpha_1 \bar{\gamma})^2)^{-\frac{4}{2}} d\alpha_1 \\ &= \frac{1}{(k_b-1)^3} \int_{\alpha_1=0}^{\infty} e^{-D_1^2 \alpha_1} \alpha_1^{2m} \times \left( \frac{(k_b-1)k_1^2}{((k_1+2\bar{\gamma}\alpha_1)^2)} - \frac{k_b^2(1-k_b)k_1^2}{(k_1+2k_b\bar{\gamma}\alpha_1)^2} + \frac{2k_b k_1}{(k_1+2\bar{\gamma}\alpha_1)} - \frac{2k_b^2 k_1}{(k_1+2k_b\bar{\gamma}\alpha_1)} \right) d\alpha_1 \\ &= \frac{1}{(k_b-1)^3} \left( \int_{\alpha_1=0}^{\infty} e^{-D_1^2 \alpha_1} \alpha_1^{2m} \frac{(k_b-1)k_1^2}{(k_1+2\bar{\gamma}\alpha_1)^2} d\alpha_1 - \int_{\alpha_1=0}^{\infty} e^{-D_1^2 \alpha_1} \alpha_1^{2m} \frac{2k_b^2(1-k_b)k_1^2}{(k_1+2k_b\bar{\gamma}\alpha_1)^2} d\alpha_1 \right) \\ &\quad + \int_{\alpha_1=0}^{\infty} e^{-D_1^2 \alpha_1} \alpha_1^{2m} \frac{2k_b k_1}{(k_1+2\bar{\gamma}\alpha_1)} d\alpha_1 - \int_{\alpha_1=0}^{\infty} e^{-D_1^2 \alpha_1} \alpha_1^{2m} \frac{2k_b^2 k_1}{(k_1+2k_b\bar{\gamma}\alpha_1)} d\alpha_1 \\ &= \frac{(D_1^2)^{-(2m+1)}}{(k_b-1)^3} \left( (k_b-1) \int_{y=0}^{\infty} \left(1 + \frac{2\bar{\gamma}}{k_1 D_1^2} y\right)^{-2} e^{-y^2} dy - k_b^2(1-k_b) \int_{y=0}^{\infty} \left(1 + \frac{2k_b\bar{\gamma}}{k_1 D_1^2} y\right)^{-2} e^{-y^2} dy \right) \\ &\quad + 2k_b \int_{y=0}^{\infty} \left(1 + \frac{2\bar{\gamma}}{k_1 D_1^2} y\right)^{-1} e^{-y^2} dy - k_b^2 \int_{y=0}^{\infty} \left(1 + \frac{2k_b\bar{\gamma}}{k_1 D_1^2} y\right)^{-1} e^{-y^2} dy \end{aligned} \quad (28)$$

$$\begin{aligned} F(\bar{\gamma}) &= \frac{(D_1^2)^{-(1)}}{(k_b-1)^3} \left( (k_b-1) M\left(\frac{2\bar{\gamma}}{k_1 D_1^2}, 1, 2\right) - k_b^2(1-k_b) M\left(\frac{2k_b\bar{\gamma}}{k_1 D_1^2}, 1, 2\right) \right) \\ &\quad + 2k_b M\left(\frac{2\bar{\gamma}}{k_1 D_1^2}, 1, 1\right) - 2k_b^2 M\left(\frac{2k_b\bar{\gamma}}{k_1 D_1^2}, 1, 1\right) \\ &\quad \times \frac{(D_1^2)^{-(1)}}{(k_b-1)^3} \left( (k_b-1) \frac{1}{2\bar{\gamma}} - k_b^2(1-k_b) \frac{1}{k_1 D_1^2} \right) \\ &\quad \times \frac{1}{\frac{2k_b\bar{\gamma}}{k_1 D_1^2}} + 2k_b \frac{\ln\left(\frac{2\bar{\gamma}}{k_1 D_1^2}\right)}{\left(\frac{2\bar{\gamma}}{k_1 D_1^2}\right)} - 2k_b^2 \frac{\ln\left(\frac{2k_b\bar{\gamma}}{k_1 D_1^2}\right)}{\left(\frac{2k_b\bar{\gamma}}{k_1 D_1^2}\right)} \\ &= \frac{1}{(k_b-1)^3} \left( \frac{(k_b-1)k_1}{2\bar{\gamma}} - \frac{k_b(1-k_b)k_1}{2\bar{\gamma}} \right) \\ &\quad + \frac{k_b k_1}{\bar{\gamma}} \ln\left(\frac{2\bar{\gamma}}{k_1 D_1^2}\right) - \frac{k_b k_1}{\bar{\gamma}} \ln\left(\frac{2k_b\bar{\gamma}}{k_1 D_1^2}\right) \\ &= \frac{1}{(k_b-1)^3} \left( \frac{(k_b-1)k_1^2}{2\bar{\gamma}} - \frac{k_b k_1 \ln(k_b)}{\bar{\gamma}} \right) \\ &= \left( \frac{k_1^2}{2(k_b-1)^2} - \frac{k_b k_1 \ln(k_b)}{(k_b-1)^3} \right) \bar{\gamma}^{-1}. \end{aligned} \quad (29)$$

$$G_i(\bar{\gamma}, m > 0) = \sum_{m=1}^{\infty} \frac{D_1 D_3^{2m}}{(m!)^2} \left( \frac{D_1^{2-4m}}{2(k_b-1)^2} (k_1^2(2m-2)!) \bar{\gamma}^{-2} \right).$$



$$\begin{aligned}
F_{\bar{\gamma}} &= \frac{(D_1^2)^{-(2m+1)}}{(k_b - 1)^3} (k_b - 1) M\left(\frac{2\bar{\gamma}}{k_1 D_1^2}, 2m + 1, 2\right) - k_b^2 (1 - k_b) M\left(\frac{2k_b \bar{\gamma}}{k_1 D_1^2}, 2m + 1, 2\right) \\
&\quad + 2k_b M\left(\frac{2\bar{\gamma}}{k_1 D_1^2}, 2m + 1, 1\right) - 2k_b^2 M\left(\frac{2k_b \bar{\gamma}}{k_1 D_1^2}, 2m + 1, 1\right) \\
&= \frac{(D_1^2)^{-(2m+1)}}{(k_b - 1)^3} \left( (k_b - 1) \frac{(2m - 2)!}{\left(\frac{2\bar{\gamma}}{k_1 D_1^2}\right)^2} - k_b^2 (1 - k_b) \frac{(2m - 2)!}{\frac{2k_b \bar{\gamma}}{k_1 D_1^2}} \right. \\
&\quad \left. + 2k_b \frac{(2m - 1)!}{\left(\frac{2\bar{\gamma}}{k_1 D_1^2}\right)} - 2k_b^2 \frac{(2m - 1)!}{\left(\frac{2k_b \bar{\gamma}}{k_1 D_1^2}\right)} \right) \tag{31} \\
&= \frac{(D_1^2)^{-(2m+1)}}{(k_b - 1)^3} \left( (k_b - 1) (D_1^2) \left(\frac{k_1}{2\bar{\gamma}}\right)^2 (2m - 2)! - (1 - k_b) \left(\frac{k_1}{2\bar{\gamma}}\right)^2 (D_1^2)^2 (2m - 2)! \right. \\
&\quad \left. + \frac{k_b k_1}{\bar{\gamma}} D_1^2 (2m - 1)! - \frac{k_b k_1}{\bar{\gamma}} (D_1^2) (2m - 1)! \right) \\
&= \frac{D_1^{2-4m}}{2(k_b - 1)^2} \left( 2 \left(\frac{k_1}{2\bar{\gamma}}\right)^2 (2m - 2)! \right) \\
&= \frac{D_1^{2-4m}}{2(k_b - 1)^2} (k_1^2 (2m - 2)!) \bar{\gamma}^{-2}.
\end{aligned}$$